Drug Delivery and Translational Research (2020) 10:1122–1135
https://doi.org/10.1007/s13346-020-00752-1

ORIGINAL ARTICLE

A remarkable in vitro cytotoxic, cell cycle arresting and proapoptotic characteristics of low-dose mixed micellar simvastatin combined with alendronate sodium

Sandip A. Bandgar[1,2] · Namdeo R. Jadhav[2] · Arehalli S. Manjappa[3]

Published online: 27 March 2020

Abstract

The objective of the present study was to screen the effect of increased simvastatin (SVS) solubility, through mixed micelles as a model approach, on in vitro anticancer efficacy in combination with hydrophilic alendronate sodium (ADS) as a strategy to improve therapeutic efficacy and to repositioning the existing drugs. The SVS-loaded mixed micelles (SVS-MMs) composed of TPGS and Poloxamer-407 were prepared using the film dispersion method and characterized for SVS loading and mean particle size. The optimized SVS-MMs were physically mixed with plain ADS (SVS + ADS MMs) and screened for in vitro cytotoxicity using MTT assay and cell cycle arresting and apoptotic activities using FACS technique. The optimized SVS-MMs showed maximum SVS loading (97.3 ± 2.3%) with minimum particle size (206 ± 8 nm). The SVS + ADS MM treatment significantly ($P < 0.001$) inhibited the cell growth with low IC_{50} values against all cells (A549: 0.037 ± 0.028 μg/mL, MDAMB-231: 0.172 ± 0.031 μg/mL, PC-3: 0.022 ± 0.015 μg/mL). Further, the SVS + ADS MM treatment significantly inhibited the cell multiplication in the S phase and resulted in high % of late apoptotic and necrotic cells at low concentration (0.05 and 0.15 μg/mL) as compared other test samples. The above results revealed the significance of encapsulating SVS in the core of MMs (improved solubility), and high efficacy and quick effect of SVS + ADS MM treatment against all cell lines screened.

Keywords Simvastatin · Bisphosphonate · Mixed micelles · Cytotoxicity · Cell cycle arresting and apoptosis

Introduction

Statins [3-hydroxy-3-methylglutaryl-CoA (HMG-CoA) reductase inhibitors], clinically used to reduce blood cholesterol levels, are the second-most prescribed drugs after analgesics and are also considered to be among the safest drugs [1]. In cell-based experiments (in vitro and experimental animal models), the hydrophobic statins (simvastatin, lovastatin, and fluvastatin) have displayed inhibitory effects on many cancers [1, 2]. Schmidmaier et al. have proved (in phase II clinical study) the pivotal role of simvastatin (SVS) in reducing drug resistance by inhibition of HMG-CoA reductase and antimyeloma activity in humans [3]. Besides, many researchers are investigating SVS in clinic for the treatment and management of various cancers and associated metastasis (https://clinicaltrials.gov/).

Nitrogen-containing bisphosphonates (NBPs; alendronate sodium (ADS)) have been proved to reduce and delay bone complications from bone metastasis, and have been used in over 4 million patients worldwide for the treatment of bone metastasis from solid tumors, bone complications, and pain from multiple myeloma. In the clinic, NBPs have been demonstrated additional direct anticancer effects [4].

SVS and ADS are known to affect cholesterol metabolism and biosynthesis by inhibiting the mevalonate pathway via potentially inhibiting the critical enzymes of the mevalonate pathway (HMG-CoA reductase and farnesyl pyrophosphate synthase (FPPS) respectively), thus having the negative effects at

Electronic supplementary material The online version of this article (https://doi.org/10.1007/s13346-020-00752-1) contains supplementary material, which is available to authorized users.

✉ Namdeo R. Jadhav
nrjadhav18@rediffmail.com

[1] Department of Pharmaceutics, Ashokrao Mane College of Pharmacy, Peth Vadgaon, Maharashtra 416112, India

[2] Department of Pharmaceutics, Bharati Vidyapeeth College of Pharmacy, Kolhapur, Maharashtra 416013, India

[3] Department of Pharmaceutics, Tatyasaheb Kore College of Pharmacy, Warananagar, Maharashtra 416113, India

various levels on cancer cells. The simultaneous inhibition of these enzymes, using a combination of these two drugs, may result in an amplified anticancer effect and allow for use of significantly lower doses of the drugs involved. Further, because of the bone-anabolic properties of SVS [5–8] and antiresorptive/bone-targeting characteristics of ADS [4, 9, 10], this combination would be more effective to treat bone cancers (multiple myeloma, osteosarcoma, etc.), bone metastasis, and associated symptoms like bone loss and pain [11].

In earlier studies, this combination was tested for synergistic anticancer effect [12], preventing periodontitis bone loss [13], in patient with polycythemia vera [14], and anti-osteoporotic and anti-atherogenic effects [15]. All these studies have proved the remarkable effect of the combination therapy than monotherapy. However, the detailed study on the combination anticancer effect of these two plain and nanoparticulate drugs is not been reported and validated. Thus, in the present study, we have attempted to screen and validate the combination anticancer effect of these two drugs.

Polymeric micelle systems, among many nanocarrier systems, were recognized as one of the most promising strategies to deliver poorly soluble drugs like SVS. Poorly soluble drugs can be made soluble within the hydrophobic inner core of a micelle and hydrophilic shell interface the biological media. As a result, micelles can substantially improve the solubility and bioavailability of various hydrophobic drugs [16]. Besides, the nanosized micelles show increased drug cell uptake, decreased drug cell efflux, increased drug circulation half-life, and a higher delivery of encapsulated drugs to tumors via the enhanced permeability and retention effect. Further, the mixed micelles (MMs) prepared from two or more chemically different copolymers have revealed remarkable physicochemical and biopharmaceutical characteristics as compared to single copolymer micelles [17]. Thus, in the present study, the SVS-loaded MMs using two chemically different block copolymers (D-α-tocopherol polyethylene glycol 1000 succinate (TPGS) and Poloxamer-407 (P-407)) were prepared to improve the SVS aqueous solubility and to study the effect of increased SVS micellar solubility on in vitro anticancer effect when physically mixed with hydrophilic ADS (SVS + ADS MMs). We hypothesize that the MMs containing SVS in the core and the hydrophilic ADS in the water surrounding the micelles and water present in the corona would improve the cellular uptake of these two drugs through endocytosis and results in amplified in vitro cytotoxicity.

Materials and methods

Materials

Simvastatin was gifted by Tocris Bio-Techne Mumbai, India. Poloxamer-407 was gifted by BASF, India. Alendronate sodium, TPGS, Annexin V-FITC, and propidium iodide (PI) were purchased from Sigma-Aldrich, Mumbai. India. DMEM, RPMI, FBS, PenStrep, and trypsin were procured from Invitrogen, India. MTT (thiazolyl blue tetrazolium bromide) was purchased from Himedia, India. All other reagents used were of analytical reagent grade and were used without further purification.

Cell culture

Human triple-negative breast adenocarcinoma (MDA MB-231: derived from the metastatic site, pleural effusion), human prostate adenocarcinoma (PC-3: derived from the metastatic site, bone), and human lung adenocarcinoma (A549) cell lines were procured from ATCC, USA. The stock cells were cultured in DMEM and RPMI supplemented with 10% inactivated fetal bovine serum (FBS), penicillin (100 IU/mL), and streptomycin (100 μg/mL) in a humidified atmosphere of 5% CO_2 at 37 °C. The cells were dissociated with cell dissociating solution (0.2% trypsin, 0.02% EDTA, and 0.05% glucose in PBS).

Determination of critical micellar concentration

The critical micellar concentration (CMC) of TPGS, P-407, and their binary mixture (1:1 M ratio) was determined using the iodine UV spectroscopy method [18–20]. The standard potassium iodide (KI)/iodine (I_2) solution was prepared by dissolving I_2 (1 g) and KI (2 g) in deionized water (100 mL). The molar solutions of TPGS, P-407, and binary mixtures were prepared in deionized water (0.05, 0.1, 0.2, 0.3, 0.4, 0.5, 0.6, 0.7, and 0.8 mM). To each copolymer solution, standard KI/I_2 solution (25 μL) was added and incubated for 12 h in dark at room temperature. Then, absorbance was read at 366 nm using a UV-Visible spectrophotometer (Double beam Shimadzu 1900, Japan). The I_2 absorption intensity was plotted against the logarithm of copolymer concentration, and CMC was determined from the graph. The sharp increase in iodine intensity indicates the formation of micelles.

Preparation of SVS-loaded mixed micelles

SVS-loaded TPGS and P-407 mixed micelles (SVS-MMs) were prepared using the film dispersion method [21]. The MMs were prepared at varied molar ratios of TPGS and P-407 (Table 1). Briefly, accurately weighed quantities of SVS, TPGS, and P-407 were dissolved in beakers containing 5 mL of methanol. The solvent was then evaporated at room temperature and the resultant film at the bottom of beaker was redispersed with 10 mL of double-distilled water using bath sonicator (5 min). The resultant solution was then centrifuged at 5000 rpm for 10 min and the supernatant mixed micellar solution was recovered and used for further analysis. The

Table 1 % entrapment efficiency, % loading capacity, and mean particle size of MMs prepared at different molar ratios of TPGS and P-407

MMs composition (SVS:TPGS:P-407)	% entrapment efficiency	% loading capacity	Mean particle size (nm)
1:1:1 (0.011:0.011:0.011 mM)	97.3 ± 2.3****	3.09 ± 0.13****	206 ± 8*
1:2:1 (0.011:0.022:0.011 mM)	86.7 ± 3.3	2.49 ± 0.24	210 ± 15
1:1:2 (0.011:0.011:0.022 mM)	70.5 ± 1.9	1.21 ± 0.09	247 ± 11

Values presented are mean ± SD, $n = 3$

****$P < 0.0001$ when compared to MMs prepared with 1:2:1 and 1:1:2 M ratios. *$P < 0.05$ when compared to MMs prepared with 1:1:2 M ratio

optimized SVS-MMs (based on entrapment and particle size) were then mixed physically with ADS at a weight equivalent to loaded SVS (SVS + ADS MMs) and used for in vitro anticancer assays.

Characterization of SVS-MMs

The 0.2 mL of the supernatant micellar solution was dissolved up to 10 mL with methanol and absorbance was read against respective blank mixed micelles in methanol using UV-Visible spectrophotometer. The % entrapment efficiency (%EE) and % loading capacity (%LC) were calculated using the below mentioned formulae.

$$\%EE = \frac{\text{Amount of drug recovered}}{\text{Amount of drug added}} \times 100$$

$$\%LC = \frac{\text{Amount ofdrug recovered}}{\text{Amount formulation components (Drug + Excipients)}} \times 100$$

The mean particle size and zeta potential of prepared SVS-MMs were determined using Horiba particle size and zeta potential analyzer (HORIBA SZ-100) (HORIBA Scientific Ltd. Japan). The measurements were performed in triplicate at 25 °C.

The micelle formation was confirmed by transmission electron microscope (TEM, FEI Tecnai T-20ST) analysis. Few drops of micellar solutions were placed on to the copper grid, air-dried, and then negative stained with 2% w/v phosphotungstic acid solution. The samples were then air-dried again and observed under TEM to understand the self-assembling nature and surface morphology of SVS-MMs [22].

In vitro cytotoxicity using MTT assay

Briefly, 100 μL of cell suspension was added to each well of the 96-well microtiter plate (50,000 cells/well). After 24-h incubation, the supernatant from each well was replaced with 100 μL of different concentrations of test drugs. The plates were then incubated at 37 °C for 24 h in a 5% CO_2 atmosphere. After incubation, the test solutions in the wells were replaced with 100 μL of MTT solution (0.05 mg) and plates were incubated at 37 °C in a 5% CO_2 atmosphere for 4 h. The MTT solution was replaced with DMSO (100 μL) and plates were gently shaken to solubilize the formed formazan crystals. The absorbance was then measured using a microplate reader at a wavelength of 590 nm. The % growth inhibition was calculated, and the concentration of test drug needed to inhibit 50% cell growth (IC_{50}) is generated from the dose-response curves for each cell line [22, 23].

Cell cycle arresting behavior using FACS

1×10^6 cells were seeded and cultured for 24 h in a 6-well plate containing 2 mL of media. Cells were then incubated with drug solutions (2 mL) prepared in complete media for 24 h. Cells were then harvested and centrifuged at 2000 rpm for 5 min at room temperature and the supernatant was discarded carefully retaining the cell pellet. The cell pellet was washed twice by resuspending in 2 mL of 1X PBS. Cells were then fixed by resuspending in 300 μL of sheath fluid followed by the addition of 1 mL of chilled 70% EtOH drop by drop with continuous gentle shaking, and another 1 mL of chilled 70% EtOH was added at once. The cells were then stored at 4 °C overnight and centrifuged at 2000 rpm for 5 min and the pellet was washed twice with cold 1X PBS (2 mL). The cell pellet was then resuspended in 450 μL of sheath fluid containing 0.05 mg/mL PI and 0.05 mg/mL RNase A and incubated for 15 min in dark. The percentage of treated and untreated cell populations in various stages of the cell cycle was determined using FACS Caliber (BD Biosciences, San Jose, CA). The standard colchicine (25 μM) was used as a positive control and a minimum of 10,000 cells were acquired for each sample [23, 24].

Apoptosis study

1×10^6 cells per well were seeded into a 6-well plate. After 24 h, the floating (dead) cells were transferred into 15-mL tubes. The cell suspension was then centrifuged, and cells were washed twice with cold PBS and then resuspended in 1 mL of 1X that were removed by replacing old culture medium with a new medium of the same volume containing drug solutions. After 24 h of incubation, the culture medium along with the binding buffer was at a concentration of $\sim 1 \times 10^6$

cells/mL. Then, 500 μL of cell suspension was aliquoted and 10 μL of PI and 5 μL Annexin V were added. The suspension was then incubated for 15 min at room temperature in the dark. Post incubation, the cells were analyzed by flow cytometer as soon as possible (within 1 h). The standard doxorubicin (25 μM) was used as a positive control and a minimum of 10,000 cells were acquired for each experimental setup [23, 24].

General settings of FACS analysis Linear and log settings in the detectors and amps window were adjusted. Voltages were set accordingly. Fluorescence channels for cell surface staining should be log. Cell cycle fluorescence should be linear. Hence, FSC and SSC are usually run on linear scale for cell cycle arrest and log scale for apoptosis study. This was used to identify single cell count. PI was detected with emission at 620 nm and Annexin V-FITC was detected at emission range of 528 nm.

Statistical analysis

Data are presented as the mean ± standard deviation of three independent experiments. GraphPad Prism software version 8 (GraphPad Software, Inc., La Jolla, CA, USA) was used for statistical analysis. The obtained results were analyzed using one-way ANOVA and $P < 0.05$ was considered to indicate a statistically significant difference.

Results and discussion

Poloxamer-407 (P-407), a US FDA-approved amphiphilic block copolymer of poly(ethylene oxide) (PEO) and poly(-propylene oxide) (PPO), is most attractive due to its biocompatibility and low toxicity. The PPO forms the hydrophobic core and solubilize the hydrophobic drug in aqueous media, while the hydrophilic PEO corona maintains the dispersion stability of micelles [25, 26]. TPGS, an amphiphilic block copolymer derived from vitamin E (α-tocopherol) and polyethylene glycol 1000, has been widely used in the pharmaceutical field as a solubilizer, absorption enhancer, and a vehicle for lipid-based drug delivery formulations. Besides, the succinate esters of vitamin E are potent proapoptotic agents selective for cancer cells. In addition to all the above properties, both P-407 and TPGS have a widely proven activity as efflux pump inhibitors (P-glycoprotein (P-gp)); thus, they inhibit P-gp-mediated multidrug resistance [26–28]. Taking the advantages of P-407, TPGS, and their MMs (which show superior physicochemical and biopharmaceutical properties over single copolymer micelles), the present study was aimed to prepare MMs using chemically different block copolymers (P-407 and TPGS).

Fig. 1 **a–c** The absorbance intensity of I_2 has been plotted as a function of copolymer concentration and a sharp increase in I_2 intensity against copolymer concentration confirms the micelle formation

Determination of CMC

In the iodine UV spectroscopy method, the micelle formation was determined by using I_2 as a hydrophobic probe. Solubilized I_2 prefers to participate in the hydrophobic microenvironment of amphiphilic copolymers, causing the conversion of I_3^- to I_2 from the excess KI in the solution, to maintain the saturated aqueous concentration of I_2 [29]. To determine CMC, the absorbance intensity of I_2 has been plotted as a function of copolymer concentration and a sharp increase in I_2 intensity against copolymer concentration confirms the micelle formation (Fig. 1a–c). The lower CMC value was observed for TPGS (0.11 ± 0.021 mM) (Fig. 1b) as compared P-407 (0.32 ± 0.034 mM) (Fig. 1a). The CMC value of TPGS and P-407 binary mixture is found to be intermediate between the CMC of individual copolymers (0.23 ± 0.012 mM) (Fig. 1c) and this suggests favorable hydrophobic interactions between both copolymers and therefore true co-micellization. The reduced CMC value would improve the stability of MMs and provide great resistance to dissociation even upon dilution by the much larger volume of blood. Further, these results are within the range of values reported in the previous works [18, 30, 31].

SVS-MMs prepared at 1:1:1 M ratio showed high drug loading and minimum particle size

In the current study, the SVS-MMs are prepared using the film dispersion method. The effects of different molar ratios of TPGS and P-407 on %EE, %LC, and mean particle size are characterized and presented in Table 1. The SVS entrapment was determined using a UV-Visible spectrometer against corresponding blank MMs to avoid interference caused by the copolymers (TPGS and P-407) present along with the SVS [19]. Among different molar ratios, the MMs prepared with 1:1:1 mM showed almost complete entrapment of SVS in the lipophilic core (97.3 ± 2.3%) as compared to other ratios which showed significantly less %EE and %LC (Table 1).

Further, the SVS-MMs prepared at 1:1:1 M ratios showed consistent ($n = 3$), significantly small and single particle size peak (206 ± 8 nm, PDI: 0.182 ± 0.081) (Fig. 2a) as compared to other molar ratios which showed multiple particle size peaks which may be corresponding to individual copolymers and larger aggregates. Further, the small particle size observed with 1:1:1 M ratio is in accordance with the previous report [18]. Besides, the 1:1:1 mM MMs showed average zeta potential of − 17.3 ± 1.8 mV (Fig. 2b) and is found decreased to − 1.7 ± 0.6 mV when the P-407 ratio is increased (1:1:2 mM) and is restored (− 15.7 ± 3.7 mV) when the TPGS ratio is

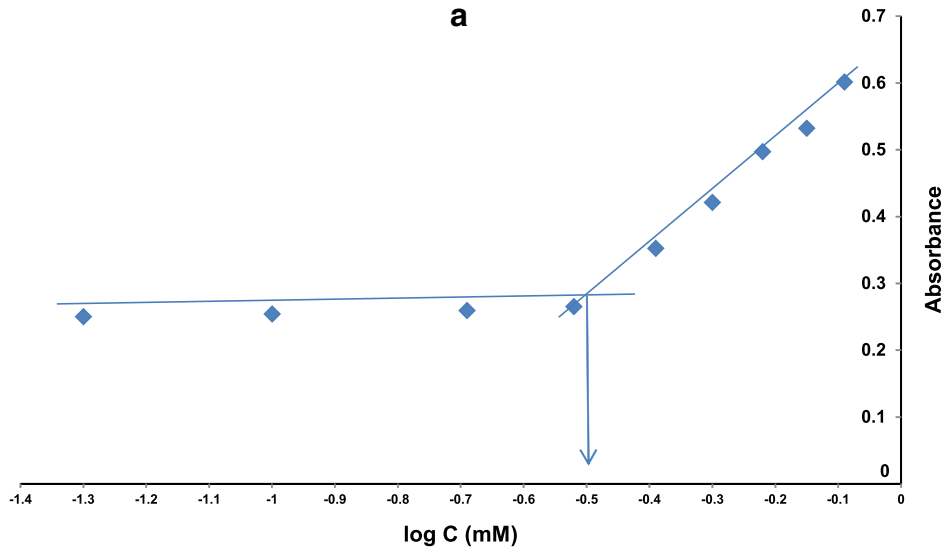
a
0.7
0.6
0.5
0.4
0.3
0.2
0.1
0
Absorbance
-1.4 -1.3 -1.2 -1.1 -1 -0.9 -0.8 -0.7 -0.6 -0.5 -0.4 -0.3 -0.2 -0.1 0
log C (mM)

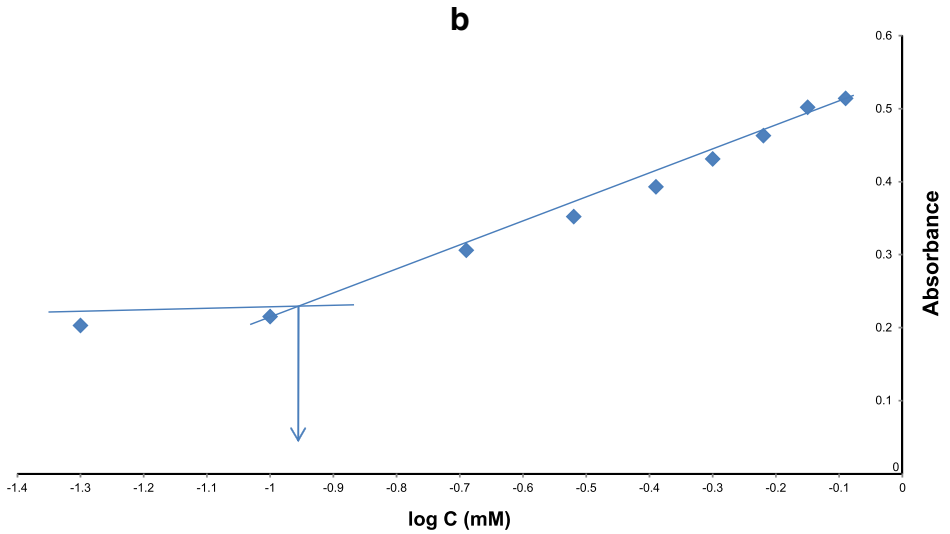
b
0.6
0.5
0.4
0.3
0.2
0.1
0
Absorbance
-1.4 -1.3 -1.2 -1.1 -1 -0.9 -0.8 -0.7 -0.6 -0.5 -0.4 -0.3 -0.2 -0.1 0
log C (mM)

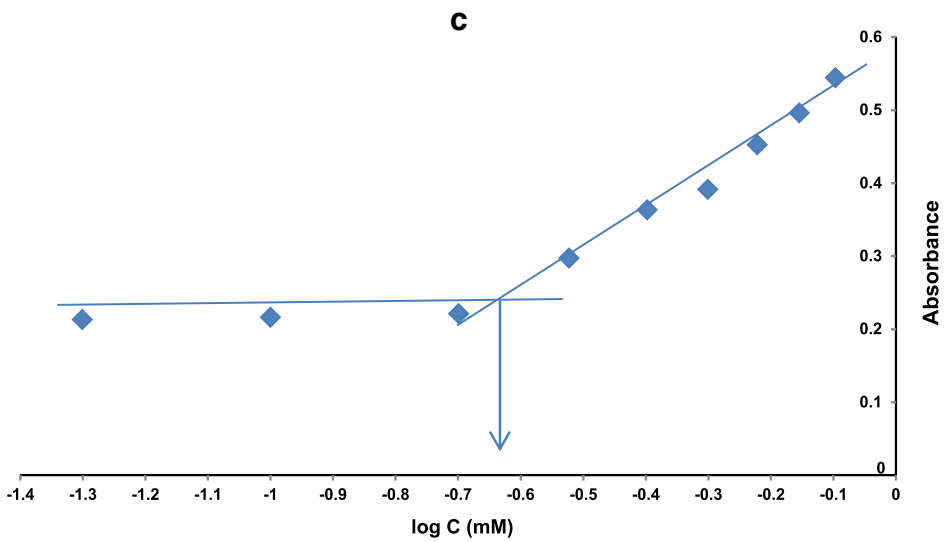
c
0.6
0.5
0.4
0.3
0.2
0.1
0
Absorbance
-1.4 -1.3 -1.2 -1.1 -1 -0.9 -0.8 -0.7 -0.6 -0.5 -0.4 -0.3 -0.2 -0.1 0
log C (mM)

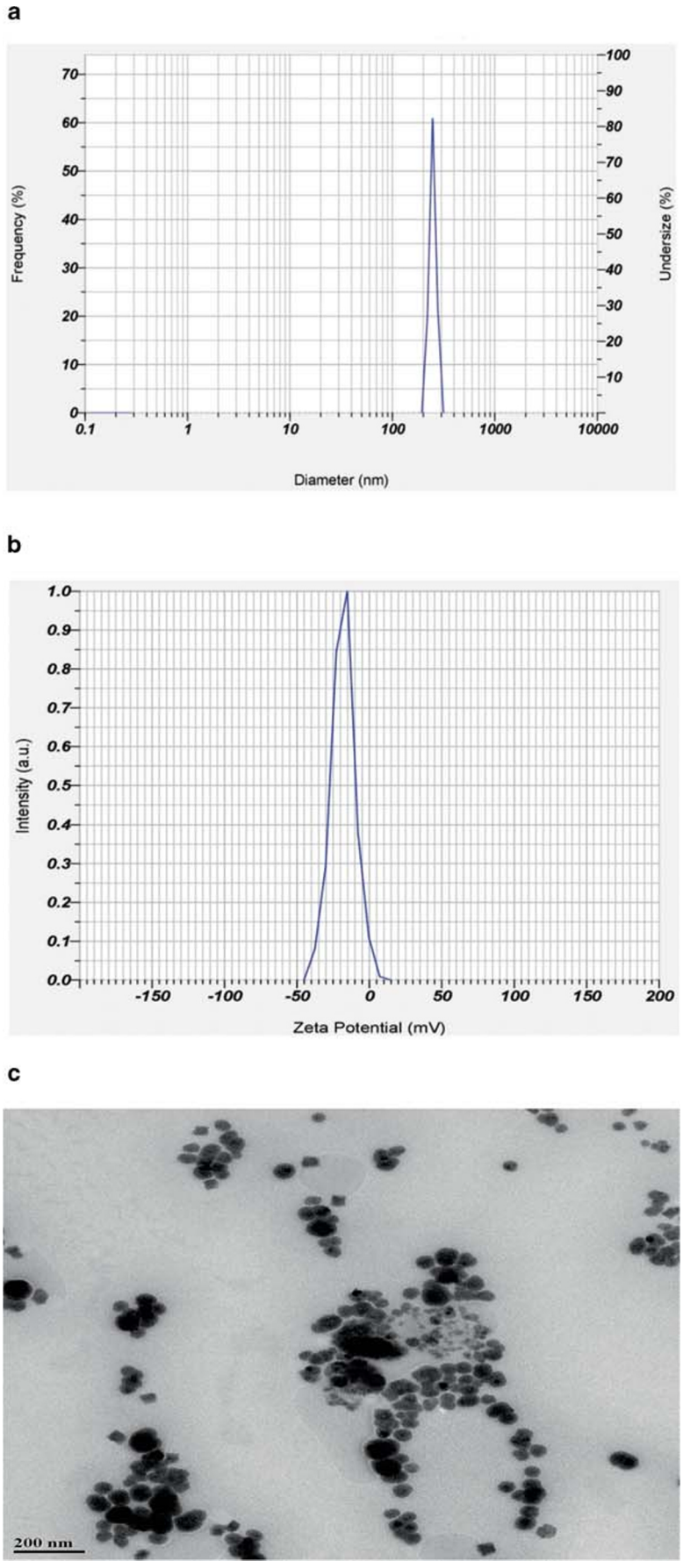

Fig. 2 **a** The SVS-MMs prepared at 1:1:1 M ratios showed consistent ($n = 3$), significantly small and single particle size peak. **b** The 1:1:1 mM MMs showed average zeta potential of − 17.3 ± 1.8 mV. **c** The TEM image of optimized SVS-MMs confirmed the moderately aggregated and spherical-shaped micellar system

increased (1:2:1 mM). These observations indicate the negative zeta potential is TPGS dependent and the increase in P-407 (the high molecular weight and linear copolymer) concentration may shield the zeta potential of low molecular weight TPGS. Based on the above obtained results, the 1:1:1 (SVS:SVS:TPGS:P-407) ratio is considered as the best composition, among other ratios tested, to prepare SVS-MMs with maximum %EE, %LC, and minimum particle size.

The objective of the TEM analysis was to confirm the micelle (aggregates) formation from the TPGS and P-407 in the aqueous medium. The TEM image of optimized SVS-MMs confirmed the moderately aggregated and spherical-shaped micellar system (Fig. 2c). It also showed the size of micelles is almost uniform (excluding larger aggregates). In the current study, the optimized SVS-MMs were physically mixed with ADS (SVS + ADS MMs) and used for further in vitro anticancer activity screening. Using TEM, it is very difficult to confirm the position of drug/s in the micelles (core and corona). However, in the physical mixture, the hydrophilic ADS would present (in the molecular state) in the water surrounding the micelles and the water present in the hydrophilic corona.

SVS + ADS MMs displayed significantly high cytotoxicity and lowest IC_{50} values against all cell lines tested

Bone is the third most frequent site of metastasis, behind lung and liver. Prostate and breast cancers are responsible for the majority of the skeletal metastases (up to 70%). The relative incidence of bone metastasis in patients with breast cancer is 65–75%, in prostate cancer is 60%, and in lung cancer is 40% [32]. Therefore, in the current study, the anticancer efficacy of SVS + ADS combination (as this combination may show the added advantages of increased anticancer, bone targeting, and bone anabolic characteristics) is screened and validated against human cancer cells (A549, MDA-MB-231, and PC-3) which most likely spread to the bone.

The effect of SVS, ADS, SVS + ADS (1:1 ratio in DMSO), and SVS + ADS MMs (1:1 ratio) on % cell growth is shown in Fig. 3. The SVS and ADS ratios taken in DMSO and in SVS + ADS MMs are same (1:1 ratio) for comparison. Based on the amount of SVS encapsulated (dissolved) per milliliter of micelles, the ADS was accurately weighed and mixed with the MMs to obtain the uniform concentration of both SVS and ADS.

All tested formulations caused concentration-dependent cell growth inhibition against all cell lines tested. The A549 cells are found significantly more sensitive (at a lower concentration) to SVS treatment than ADS treatment (Fig. 3a) as compared to other two cells tested (Fig. 3b, c). The SVS + ADS (DMSO) is found significantly more cytotoxic at lower concentration, than at higher concentration, as compared to individual treatments against all cell lines tested. The SVS + ADS MM treatment significantly inhibited the growth of all cells (at all concentrations tested) as compared to all other treatments.

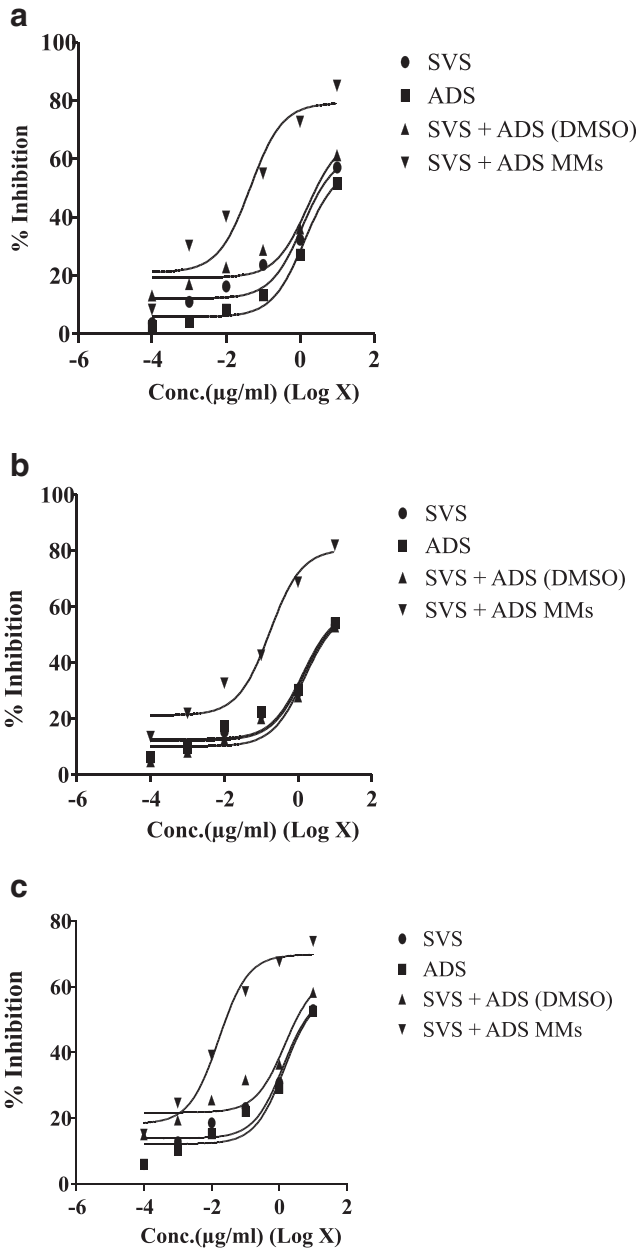

Fig. 3 **a**–**c** The effect of SVS, ADS, SVS + ADS (1:1 ratio in DMSO), and SVS + ADS MMs (1:1 ratio) on % cell growth

In the present study, the direct comparison between SVS-DMSO and SVS-MMs was not carried out to prove the effect of increased solubility via MM approach. However, the cytotoxicity of ADS-DMSO, ADS + SVS-DMSO, and ADS + SVS-MMs (SVS + ADS MMs) were compared. The increased ADS cytotoxicity when mixed with SVS-MMs than the ADS mixed with SVS in DMSO clearly indicates the utility of this formulation (SVS-MMs) and the effect of micellar solubilization of SVS.

The IC_{50} values of all formulations against tested cell lines are presented in Table 2. The IC_{50} values obtained for SVS, ADS, and SVS + ADS in DMSO are found almost similar against all cell lines indicating similar efficacy. Although SVS + ADS combination in DMSO caused moderately increased cell growth inhibition, its IC_{50} values are found almost similar to individual drug substances against all cell lines, whereas the mixed micellar SVS combined with ADS (SVS + ADS MMs) showed significantly decreased IC_{50} values against all cell lines as compared to all other formulations. These results reveal the significance of encapsulating (solubilizing) SVS in the core of MMs.

The drug-free DMSO vehicle controls, prepared in a similar way to test samples, showed no significant cell death at all DMSO concentrations equivalent to DMSO present drug solutions. However, at 0.1% v/v DMSO concentration (equivalent to DMSO present in 10 μg/mL SVS solution), the cell growth inhibition observed is in the range of 2–5% against all cell lines tested and is found to be negligible.

The cytotoxicity of empty MMs is found to be negligible (about 1–2%) at concentrations equivalent to drug-loaded micelles (ranging from 0.0001 to 1 μg/mL). However, about 11–15% cytotoxicity was noticed (against all cell lines) at empty micelle concentration equivalent to 10 μg/mL of drug-loaded micelles which indicates increased cytotoxicity of empty micelles at higher concentrations. Further, these results are in accordance with the previous reports [19, 20].

A remarkable S phase arresting is noticed with SVS + ADS MMs at low concentration (0.05 and 0.15 μg/mL)

The effects of SVS, ADS, SVS + ADS (1:1 ratio in DMSO), and SVS + ADS MMs (1:1 ratio) on cell cycle arresting and apoptosis are tested at their obtained IC_{50} values. The tested concentrations of SVS and ADS in SVS + ADS MMs for cell cycle analysis and apoptosis are less, but are present in 1:1 ratio, than the tested concentrations of SVS and ADS in DMSO (at 1:1 ratio). At a higher SVS + ADS MM concentration, equivalent to concentrations in DMSO, we observed no sufficient number of cells remained for comparison as a result of their higher cytotoxicity. Thus, the SVS + ADS MMs were tested at lower concentrations (at their IC_{50} values) for comparison.

The effects of positive control (colchicine, 25 μM) on the proliferation stages of A549, MDA-MB-231, and PC-3 cells are presented in the Supplementary Table 1. The effects of SVS, ADS, SVS + ADS (DMSO), and SVS + ADS MM treatments on proliferation phases of A549, MDA-MB-231, and PC-3 cells are presented in Fig. 4a–c. The SVS treatment resulted in about 2% and 3% more A549 cells gated in S and G2M phase respectively as compared to control cells. The ADS treatment resulted in about 7% more cells gated in S phase as compared to control cells (Fig. 4a). Further, the SVS + ADS (DMSO) treatment caused no cell arrest in both S and G2M phases; instead, it caused about 8% increased cell arrest in the G0/G1 phase as compared to control cells. In contrast to this effect, the SVS + ADS MM treatment caused significantly increased A549 cell arrest in S phase (about 25% cells) as compared to control cells. The SVS + ADS MM treatment caused about 2.46-, 3.2-, 2.0-, and 7.76-fold increased effect as compared to control cells, SVS, ADS, and SVS + ADS (DMSO) treated cells respectively.

In the current study, the formulations are also screened for their effect against MDA-MB-231 cells (Fig. 4b). The ADS treatment caused significant cell arresting in S phase (10%) and G2 phase (7%) as compared to control cells. Although the SVS treatment caused no effect on MDAMB-231 cell proliferation phases, its presence significantly potentiated the ADS effect in arresting more cells at S phase (SVS + ADS in DMSO treatment). About 7% more cells are found gated in S phase with SVS + ADS (DMSO) treatment as compared to ADS alone, whereas the SVS + ADS MMs showed significantly higher cell arresting characteristics as compared to all other formulations. It caused about 21% more cells gated in S phase as compared to SVS + ADS (DMSO) treatment.

In PC-3 cells (Fig. 4c), the SVS caused no significant effect and ADS caused about 3% more cell arrest in S phase. Further, the SVS + ADS (DMSO) treatment caused about 5% and 3% more cell arrest in the S phase and G2M phase as compared to control cells. The SVS presence does not potentiate the ADS

Table 2 IC_{50} values obtained after 24-h treatment with test substances

Formulations	IC_{50} values (μg/mL)		
	A549	MDAMB-231	PC-3
SVS	1.205 ± 0.059	1.425 ± 0.109	1.32 ± 0.108
ADS	1.295 ± 0.134	1.353 ± 0.06	1.42 ± 0.393
SVS + ADS (DMSO)	1.536 ± 0.456	1.489 ± 0.346	1.47 ± 0.31
SVS + ADS MMs	0.037 ± 0.028***$^{\theta}$	0.172 ± 0.031***$^{\theta}$	0.022 ± 0.015***$^{\theta}$

Values presented are mean ± SD, $n = 3$

****$P < 0.0001$, ***$P < 0.001$, **$P < 0.01$, and *$P < 0.05$

$^{\theta}$ P: significant when compared to all other formulations

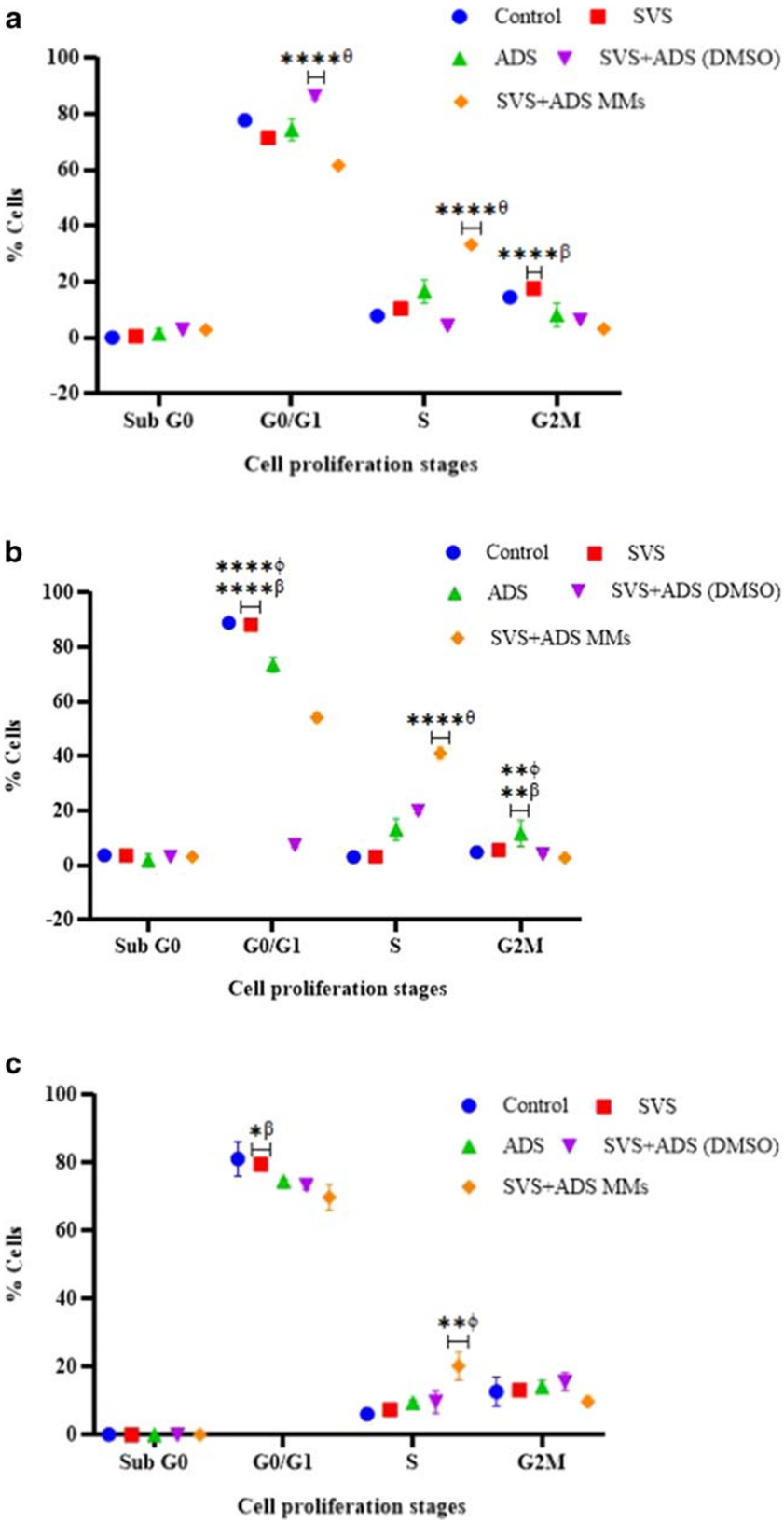

Fig. 4 **a**–**c** The effects of SVS, ADS, SVS + ADS (DMSO), and SVS + ADS MM treatments on proliferation phases of A549, MDA-MB-231, and PC-3 cells

effect as does with the MDA-MB-231 cells. However, the SVS + ADS MM treatment showed a significant effect on PC-3 cells as compared to all other formulations (about 9%

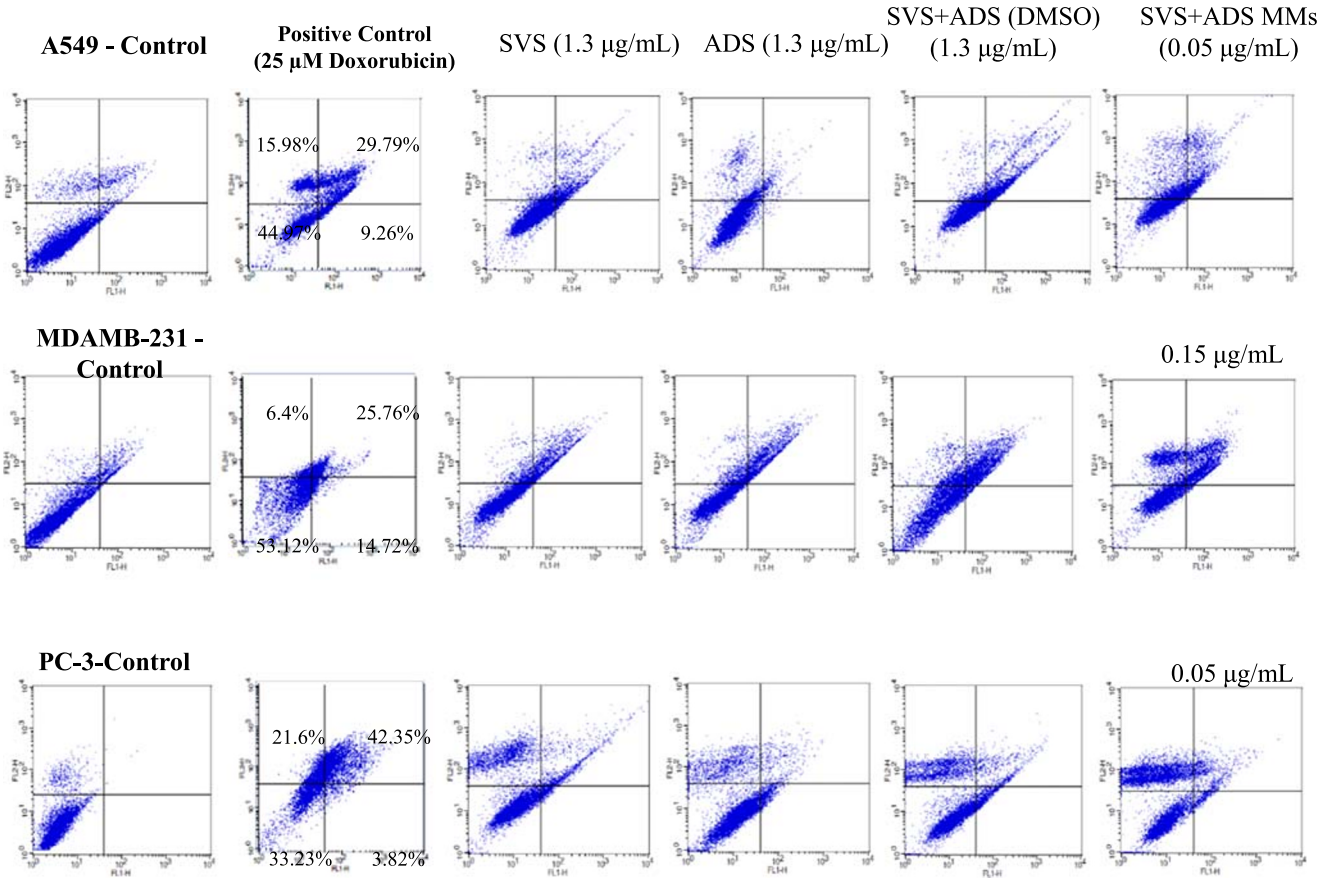

Fig. 5 The lower left (LL) square shows normal live cells, lower right (LR) shows early apoptotic cells, upper right (UR) shows late apoptotic cells, and upper left (UL) shows necrotic cells

more cells are found gated in S phase as compared to SVS + ADS in DMSO treatment).

In conclusion, the MMs caused significant cell cycle arresting against all cell lines. The MDAMB-231 cells are found more sensitive to MM treatment as compared to A549 and PC-3 cells. Similarly, SVS + ADS (DMSO) treatment is also found more effective against MDAMB-231 as compared to the other two cells.

SVS + ADS MM treatment at low concentration resulted in significantly high % of late apoptotic and necrotic cells

Apoptotic activity is always routed with translocation of phosphatidylserine (PS) from the cytosol to the cell membrane. PS specifically binds to FITC-tagged Annexin V and can be quantitatively estimated by FACS as a very specific apoptotic marker [33]. In the present study, the apoptotic activity of test substances was determined using Annexin V-FITC and propidium iodide (PI) staining method.

In Fig. 5, the lower left (LL) square shows normal live cells, lower right (LR) shows early apoptotic cells, upper right (UR) shows late apoptotic cells, and upper left (UL) shows necrotic cells. The effects of the positive control (doxorubicin, 25 µM) on A549, MDA-MB-231, and PC-3 cell apoptosis are presented in the Fig. 5 and Supplementary Table 2. The SVS treatment resulted in significantly more A549 cells (about 8%) in the late apoptotic phase as compared to control cells, whereas the ADS treatment resulted in about 12% necrotic cells (Fig. 6a). The combination effect (SVS + ADS in DMSO) is found very significant as compared to all other formulations. The SVS + ADS (DMSO) treatment caused about 2.6-fold and 10.5-fold increased A549 cells in the late apoptotic phase as compared to SVS and ADS treatments respectively, whereas the SVS + ADS MM treatment resulted in about 3.25-fold increased necrotic cells as compared to SVS + ADS (DMSO) treatment which showed about 2-fold increased cells at the late apoptotic phase as compared to SVS + ADS MMs.

In the case of MDA-MB-231 cells (Fig. 6b), the SVS, ADS, and SVS + ADS (DMSO) treatments are found more effective (resulted in high % of both late apoptotic and necrotic cells) as compared to A549 cells. The SVS and ADS combination in DMSO showed significantly more effect when compared to their individual effects, whereas the SVS + ADS MM treatment showed moderately increased % of cells (almost equal) in both late apoptotic and necrotic phases as compared to SVS + ADS (DMSO).

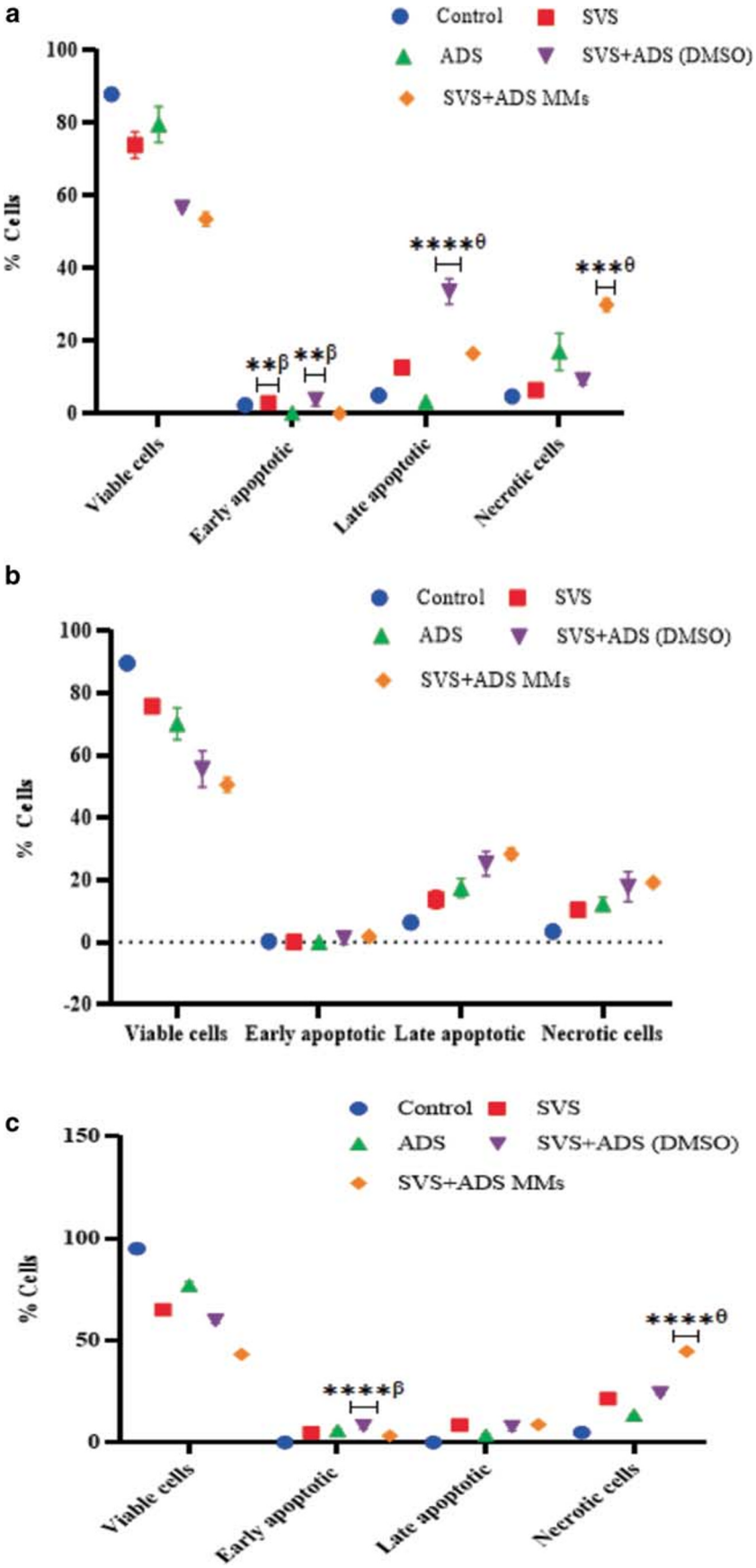

Fig. 6 **a** The SVS treatment resulted in significantly more A549 cells (about 8%) in the late apoptotic phase as compared to control cells, whereas the ADS treatment resulted in about 12% necrotic cells. **b** In the case of MDA-MB-231 cells, the SVS, ADS, and SVS + ADS (DMSO) treatments are found more effective (resulted in high % of both late apoptotic and necrotic cells) as compared to A549 cells. **c** In PC-3 cells, all formulations showed a significant effect as compared to control cells

In PC-3 cells (Fig. 6c), all formulations showed a significant effect as compared to control cells. The SVS treatment is found more effective than ADS and their combination effect in DMSO is found to be significantly high when compared to their individual effects. The % late apoptotic cells caused by SVS + ADS MMs are found almost similar to SVS + ADS (DMSO) treatment, whereas the % necrotic cells observed with SVS + ADS MM treatment are significantly high (about 1.84-fold) when compared to SVS + ADS (DMSO) treatment. These results may be correlated with quick and high effect of MMs resulting in increased necrotic cells rather late apoptotic cells. Further, these results are supported by high cytotoxic nature of MMs as shown in MTT assay.

As per the previous reports, it has been revealed that SVS stimulates cell cycle arrest and apoptosis in several cancer cell types [34] via the intracellular signaling mechanisms of RAC1 and associated downstream pathway [35, 36]. Further, the castrate-resistant prostate cancer cell (PC-3) apoptosis caused by SVS is due to inhibition of IκBα phosphorylation and nuclear translocation of p50/p65 dimer in the nuclear factor-κB pathway [37]. In other reports, the SVS and irinotecan combination treatment demonstrated a remarkable increase in PC-3 cell apoptosis via downregulation of MCL-1 levels [38] whereas SVS and sulindac combination synergistically increased the apoptotic activity and intracellular ROS production in A549 cells through AKT signaling-dependent downregulation of survivin [39]. In addition, the SVS in combination with bergamottin has potentiated the TNF-induced apoptosis through modulation of the NF-κB signaling pathway in human chronic myelogenous leukemia [40].

The all above reports reveal that the cell cycle arresting and apoptotic activity of SVS alone and in combination with other drugs are due to inhibition of different cell signaling pathways. Thus, in the present study, the observed cell cycle arresting and apoptotic effects of SVS alone and in combination with the standard proapoptotic drug, ADS, are corroborating with the above reports and are maybe due to one or all of the above reasons. Besides, the enhanced cytotoxicity could be correlated with their direct cytotoxic nature.

In the current study, a remarkable in vitro cytotoxicity, cell cycle arresting, and cell apoptosis were noticed with the very low dose of SVS-MMs combined with standard anticancer and proapoptotic drug ADS. The possible mechanisms underlying for the enhanced anticancer efficacy of low-dose SVS + ADS-MMs are increased intracellular drug accumulation as a result of increased SVS micellar solubility and cell uptake via endocytosis [18], decreased lipophilic drug (SVS) efflux, independent anticancer effects of both SVS and ADS [41], and potent proapoptotic and multidrug resistance (MDR) reversing activities of TPGS [42].

Conclusion

In the present study (preliminary examination), we have used the micelles as a model approach to improve the SVS solubility (one of the reasons reported for the poor therapeutic performance of SVS in the clinic) and check the effect of increased solubility on anticancer activity in combination with ADS which is highly water-soluble. The current study revealed the superior in vitro anticancer efficacy of SVS + ADS MMs at a very low dose over a higher concentration of individual drugs and their combination (1:1 ratio). Thus, using SVS + ADS MM approach, few of the chemotherapy hurdles such as the dose-dependent toxicity and the cost of chemotherapy could be minimized by the use of significantly lower doses of the drugs and reduced dosing frequency. However, further in vivo studies are needed with this approach to ascertain these facts. Besides, the nanoparticles co-loaded with both lipophilic (SVS) and hydrophilic (ADS) drugs (for instance, the liposomal system containing ADS in the inner aqueous phase and SVS in the lipophilic membrane or other suitable approach to co-load them in a single nanoparticle) could further increase the anticancer efficacy of this drug combination as a result of simultaneous cellular uptake of both hydrophilic and lipophilic drugs. Further, the active targeting of these nanoparticles via surface modification with ligands in a suitable animal model would be an interesting and effective approach for future study.

Acknowledgments Authors thank the Bharati Vidyapeeth College of Pharmacy, Kolhapur, for providing facility to carry out this research project. Authors also thank Ashokrao Mane College of Pharmacy, Peth Vadgaon, for supporting this research work.

Compliance with ethical standards

Conflict of interest The authors declare that they have no conflict of interest.

References

1. Kochuparambil ST, Al-Husein B, Goc A, Soliman S, Somanath PR. Anticancer efficacy of simvastatin on prostate cancer cells and tumor xenografts is associated with inhibition of Akt and reduced prostate-specific antigen expression. J Pharmacol Exp Ther. 2011;336(2):496–505.
2. Jakobisiak M, Golab J. Statins can modulate effectiveness of antitumor therapeutic modalities. Med Res Rev. 2010;30(1):102–35.
3. Schmidmaier R, Baumann P, Bumeder I, Meinhardt G, Straka C, Emmerich B. First clinical experience with simvastatin to overcome drug resistance in refractory multiple myeloma. Eur J Haematol. 2007;79(3):240–3.
4. Jiang P, Zhang P, Mukthavaram R, Nomura N, Pingle SC, Teng D, et al. Anti-cancer effects of nitrogen-containing bisphosphonates on human cancer cells. Oncotarget. 2016;7(36):57932–42.

5. Zhang Y, Bradley AD, Wang D, Reinhardt RA. Statins, bone metabolism and treatment of bone catabolic diseases. Pharmacol Res. 2014;88:53–61.
6. Oryan A, Kamali A, Moshiri A. Potential mechanisms and applications of statins on osteogenesis: current modalities, conflicts and future directions. J Control Release. 2015;215:12–24.
7. Dai L, Xu M, Wu H, Xue L, Yuan D, Wang Y, et al. The functional mechanism of simvastatin in experimental osteoporosis. J Bone Miner Metab. 2016;34(1):23–32.
8. Sequetto PL, Gonçalves RV, Pinto AS, Oliveira MGA, Maldonado IRSC, Oliveira TT, et al. Low doses of simvastatin potentiate the effect of sodium alendronate in inhibiting bone resorption and restore microstructural and mechanical bone properties in glucocorticoid-induced osteoporosis. Microsc Microanal. 2017;23(5):989–1001.
9. Rogers MJ, Crockett JC, Coxon FP, Monkkonen J. Biochemical and molecular mechanisms of action of bisphosphonates. Bone. 2011;49(1):34–41.
10. Khosla S, Bilezikian JP, Dempster DW, Lewiecki EM, Miller PD, Neer RM, et al. Benefits and risks of bisphosphonate therapy for osteoporosis. J Clin Endocrinol Metab. 2012;97(7):2272–82.
11. Kobayashi Y, Kashima H, Rahmanto YS, Banno K, Yu Y, Matoba Y, et al. Drug repositioning of mevalonate pathway inhibitors as antitumor agents for ovarian cancer. Oncotarget. 2017;8(42):72147–56.
12. Rogers M, Kalra S, Moukharskaya J, Chakraborty K, Niyazi M, Krishnan K, et al. Synergistic growth inhibition of PC3 prostate cancer cells with low-dose combinations of simvastatin and alendronate. Anticancer Res. 2015;35(4):1851–9.
13. Price U, Le HO, Powell SE, Schmid MJ, Marx DB, Zhang Y, et al. Effects of local simvastatin—alendronate conjugate in preventing periodontitis bone loss. J Periodontal Res. 2013;48(5):541–8.
14. Sørensen AL, Kallenbach K, Hasselbalch HC. A remarkable hematological and molecular response pattern in a patient with polycythemia vera during combination therapy with simvastatin and alendronate. Leuk Res Rep. 2016;6:20–3.
15. Mohamed MT, Abuelezz SA, Atalla SS, El Aziz LFA, Gorge SS. The anti-osteoporotic and anti-atherogenic effects of alendronate and simvastatin in ovariectomized rats fed high fat diet: a comparative study of combination therapy versus monotherapy. Biomed Pharmacother. 2017;89:1115–24.
16. Zhao D, Zhang H, Yang S, He W, Luan Y. Redox-sensitive mPEG-SS-PTX/TPGS mixed micelles: an efficient drug delivery system for overcoming multidrug resistance. Int J Pharm. 2016;515(1–2):281–92.
17. Manjappa AS, Kumbhar PS, Patil AB, Disouza JI, Patravale VB. Polymeric mixed micelles: improving the anticancer efficacy of single-copolymer micelles. Crit Rev Ther Drug Carrier Syst. 2019;36(1):1–58.
18. Grimaudo MA, Pescina S, Padula C, Santi P, Concheiro A, Alvarez-Lorenzo C, et al. Poloxamer 407/TPGS mixed micelles as promising carriers for cyclosporine ocular delivery. Mol Pharm. 2018;15(2):571–84.
19. Patra A, Satpathy S, Shenoy AK, Bush JA, Kazi M, Hussain MD. Formulation and evaluation of mixed polymeric micelles of quercetin for treatment of breast, ovarian, and multidrug resistant cancers. Int J Nanomedicine. 2018;13:2869–81.
20. Jadhav P, Bothirajaa C, Pawar A. Resveratrol-piperine loaded mixed micelles: formulation, characterization, bioavailability, safety and in vitro anticancer study. RSC Adv. 2016;6:112795–805.
21. Dian L, Yu E, Chen X, Wen X, Zhang Z, Qin L, et al. Enhancing oral bioavailability of quercetin using novel soluplus polymeric micelles. Nanoscale Res Lett. 2014;9(1):2406.
22. Kumbhar PS, Birange S, Atavale M, Disouza JI, Manjappa AS. D-Gluconic acid–based methotrexate prodrug-loaded mixed micelles composed of MDR reversing copolymer: in vitro and in vivo results. Colloid Polym Sci. 2018;296(12):1971–81.
23. Manjappa AS, Ramachandra Murthy RS. Unravelling the anticancer efficacy of 10-oxo-7-epidocetaxel: in vitro and in vivo results. Drug Dev Ind Pharm. 2019;45(3):474–84.
24. Ramanlal Chaudhari K, Kumar A, Megraj Khandelwal VK, Ukawala M, Manjappa AS, Mishra AK, et al. Bone metastasis targeting: a novel approach to reach bone using Zoledronate anchored PLGA nanoparticle as carrier system loaded with docetaxel. J Control Release. 2012;158(3):470–8.
25. Bodratti AM, Alexandridis P. Formulation of poloxamers for drug delivery. J Funct Biomater. 2018;9(1):E11.
26. Saxena V, Hussain MD. Poloxamer 407/TPGS mixed micelles for delivery of gambogic acid to breast and multidrug-resistant cancer. Int J Nanomedicine. 2012;7:713–21.
27. Meng X, Liu J, Yu X, Li J, Lu X, Shen T. Pluronic F127 and D-alpha-tocopheryl polyethylene glycol succinate (TPGS) mixed micelles for targeting drug delivery across the blood brain barrier. Sci Rep. 2017;7(1):2964.
28. Cambón A, Brea J, Loza MI, Alvarez-Lorenzo C, Concheiro A, Barbosa S, et al. Cytocompatibility and P-glycoprotein inhibition of block copolymers: structure-activity relationship. Mol Pharm. 2013;10(8):3232–41.
29. Wei Z, Hao J, Yuan S, Li Y, Juan W, Sha X, et al. Paclitaxel-loaded pluronic P123/F127 mixed polymeric micelles: formulation, optimization and in vitro characterization. Int J Pharm. 2009;376(1–2):176–85.
30. Bakshi MS, Sachar S. Influence of temperature on the mixed micelles of Pluronic F127 and P103 with dimethylene-bis-(dodecyldimethylammonium bromide). J Colloid Interface Sci. 2006;296(1):309–15.
31. Zhang Z, Tan S, Feng SS. Vitamin E TPGS as a molecular biomaterial for drug delivery. Biomaterials. 2012;33(19):4889–906.
32. Macedo F, Ladeira K, Pinho F, Saraiva N, Bonito N, Pinto L, et al. Bone metastases: an overview. Oncol Rev. 2017;11(1):321.
33. Susin SA, Daugas E, Ravagnan L, Samejima K, Zamzami N, Loeffler M, et al. Two distinct pathways leading to nuclear apoptosis. J Exp Med. 2000;192(4):571–80.
34. Saito A, Saito N, Mol W, Furukawa H, Tsutsumida A, Oyama A, et al. Simvastatin inhibits growth via apoptosis and the induction of cell cycle arrest in human melanoma cells. Melanoma Res. 2008;18(2):85–94.
35. Buranrat B, Suwannaloet W, Naowaboot J. Simvastatin potentiates doxorubicin activity against MCF-7 breast cancer cells. Oncol Lett. 2017;14(5):6243–50.
36. Altwairgi AK. Statins are potential anticancerous agents (review). Oncol Rep. 2015;33(3):1019–39.
37. Park YH, Seo SY, Lee E, Ku JH, Kim HH, Kwak C. Simvastatin induces apoptosis in castrate resistant prostate cancer cells by deregulating nuclear factor-κB pathway. J Urol. 2013;189(4):1547–52.
38. Alqudah MAY, Mansour HT, Mhaidat N. Simvastatin enhances irinotecan-induced apoptosis in prostate cancer via inhibition of MCL-1. Saudi Pharm J. 2018;26(2):191–7.
39. Kim YS, Seol CH, Jung JW, Oh SJ, Hwang KE, Kim HJ, et al. Synergistic effect of sulindac and simvastatin on apoptosis in lung cancer A549 cells through AKT-dependent downregulation of survivin. Cancer Res Treat. 2015;47(1):90–100.
40. Kim SM, Lee EJ, Lee JH, Yang WM, Nam D, Lee JH, et al. Simvastatin in combination with bergamottin potentiates TNF-induced apoptosis through modulation of NF-κB signalling

pathway in human chronic myelogenous leukaemia. Pharm Biol. 2016;54(10):2050–60.
41. Daria YA, Alexander VK. Pluronics and MDR reversal: an update. Mol Pharm. 2014;11:2566–78.
42. Neophytou CM, Constantinou C, Papageorgis P, Constantinou AI. D-α-tocopheryl polyethylene glycol succinate (TPGS) induces cell cycle arrest and apoptosis selectively in survivin-overexpressing breast cancer cells. Biochem Pharmacol. 2014;89:31–42.